Appl. Phys. B (2013) 113:373–378
DOI 10.1007/s00340-013-5487-1

Applied Physics B
Lasers and Optics

Excimer laser-induced diamond graphitization for high-energy nuclear applications

E. Alemanno · A. P. Caricato · G. Chiodini · M. Martino · P. M. Ossi · S. Spagnolo · R. Perrino

Published online: 6 November 2013

Abstract In this work, we have studied the structure and the morphology of a graphite layer induced on the surface of a polycrystalline thermal grade CVD diamond by focusing a pulsed excimer laser operating at KrF (wavelength 248 nm) and ArF (wavelength 193 nm) mixtures. By micro-Raman and photoluminescence spectroscopies, as well as scanning electron microscopy, we reported the synthesis of a turbostratic t-graphite layer after irradiation with ArF laser. By contrast, irradiating with a KrF laser beam, we obtained a disordered graphite layer with 10 laser shots, while 200 consecutive laser pulses resulted in target ablation.

1 Introduction

Due to its exceptional electrical, thermal and optical properties, diamond is a very attractive material for radiation detection. Diamond can detect any kind of radiation that is more energetic than its bandgap of 5.47 eV, e.g., deep UV photons, X-rays, gamma rays, charged particles and neutrons with energies ranging from 5.47 eV up to GeV of cosmic rays. Because of its radiation hardness, it needs no frequent replacements, it can work at room temperature with no need for cooling, it has a resistivity several orders of magnitude greater than silicon, it has an extremely low leakage current and no need for p-type or n-type junctions as required in silicon radiation detectors. Diamond radiation detectors are generally designed as a solid-state ionization chamber mainly in two configurations: with electrodes up and down the plate (called planar or "sandwich" configuration) or interdigitated electrodes on a surface. A charged particle, or a photon with energy higher than the bandgap, passes through the diamond and ionizes it, generating an electron-hole pairs (energy to form e-h pair: 13 eV) [1] which are separated by the electric field between the electrodes. Charge carriers are then collected by the electrodes and contribute to the current in the detector which is measured by an external circuit. In this work, we investigated the structure and the morphology of the induced graphite layer by irradiating with a focused, pulsed excimer laser, operating at KrF (wavelength 248 nm) and ArF (wavelength 193 nm), the surface of a polycrystalline thermal grade CVD diamond. The structure of the graphite layers was characterized performing micro-Raman and photoluminescence (PL) measurements along with scanning electron microscopy (SEM). The aim of this work is to realize ohmic graphite electrical contacts on the surface of the diamond plate to be used as detector in high-energy nuclear applications avoiding metal depositions on diamond surfaces.

2 Experimental

A polycrystalline thermal grade CVD diamond surface sample ($10 \times 10 \times 0.2$ mm^3) was irradiated with an excimer laser (Lambda Physik LPX 305i), emitting at two

E. Alemanno · A. P. Caricato · M. Martino · S. Spagnolo
Department of Mathematics and Physics, "E. De Giorgi", University of Salento, Via Arnesano, 73100 Lecce, Italy

E. Alemanno (✉) · A. P. Caricato · G. Chiodini · M. Martino · S. Spagnolo · R. Perrino
National Institute for Nuclear Physics (INFN), Via Monteroni, 73100 Lecce, Italy
e-mail: emanuele.alemanno@le.infn.it

P. M. Ossi
Department of Energy, Center for Nano Engineered Materials and Surfaces (NEMAS), Politecnico di Milano, Milan, Italy

wavelengths, (λ = 248 nm and λ = 193 nm). The laser emitted a 20 nsec long pulse with energy of about 160 mJ/pulse at 10-Hz repetition rate. The laser beam, with a transverse size of about 20 × 10 mm^2, was directed onto a beam homogenizer single matrix. The homogenized beam was then directed via a lens onto the sample placed on a computer-assisted XY holder with a micrometric resolution. The focused image was a square of 3 mm^2, and the laser fluence was about 5 J/cm^2 with a top-hat profile. The setup scheme is depicted in Fig. 1. The diamond plate was processed in air and at room temperature. We generated different patterns on the surface of the diamond, and for each zone, we chose different laser parameters, then we checked the material response. In Fig. 2., the different processed areas are reported: the A area was achieved while the XY motion is stopped, focusing 200 KrF consecutive laser pulses. The same experimental procedure was applied to the B area and to the B3 area. In the B area, we used only 10 laser shots, while B3 area was accidentally produced, because during the laser incidence, the sample jumped off from its holder, so it will be not considered. Finally, C area was achieved scanning the surface of the diamond plate, moving with a speed of about 0.3 mm/s, with the laser beam realizing 3 adjacent rows with a total area of about 9 mm^2. Then, we performed micro-Raman measurements on diamond and on graphite pad using an Ar^+ laser (wavelength 514.5 nm) which was focused by a 50× optical objective (Leica, Germany). The numerical aperture was 0.75, which corresponds to a spot diameter of 1 μm. The laser power at the sample surface was set at 1 mW, minimizing the possible radiation damage. The backscattered light was collected by the same objective and analyzed by a Renishaw InVia Raman Microscope equipped with a holographic Notch filter (cut-off at 100 cm^{-1}), a 1,800 lines/mm diffraction grating and a thermoelectrically cooled RenCam CCD detector. The resolution was 0.5 cm^{-1} in the wavenumber range from 100 to 8,000 cm^{-1}. Raman spectra were taken at different points of the graphite pad areas in order to evaluate spectra reproducibility. For A area, we collected two Raman spectra at two different positions named KrFA1 and KrFA2, respectively. For B area, we have the points KrFB1 and KrFB2. For C area, we have divided the stripe into two halves, the spectra were recorded at two positions (points ArFC1 and ArFC2), located at the stripe center, at a distance of about one-sixth of the stripe length from the external border on both sides. Additionally, we performed photoluminescence (PL) measurements on CVD diamond and on graphite layer. In order to confirm the micro-Raman and PL results, we also performed scanning electron microscopy by means of a field ion microscope (Zeiss Supra-40) gently using a silver layer metallizing the sample, thus allowing the observations at higher magnifications on the insulating material.

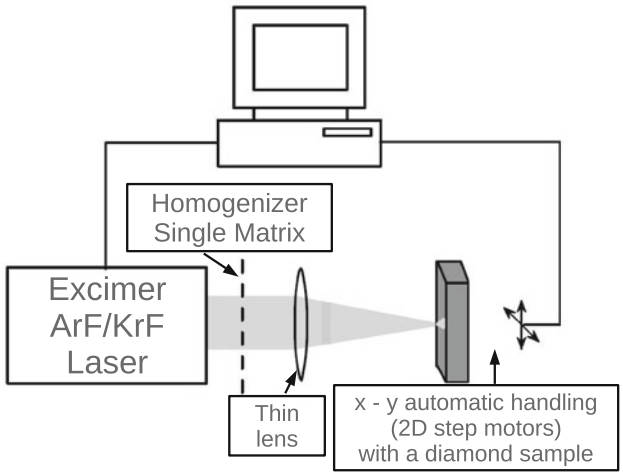

Fig. 1 Scheme of the setup for irradiating a diamond plate surface

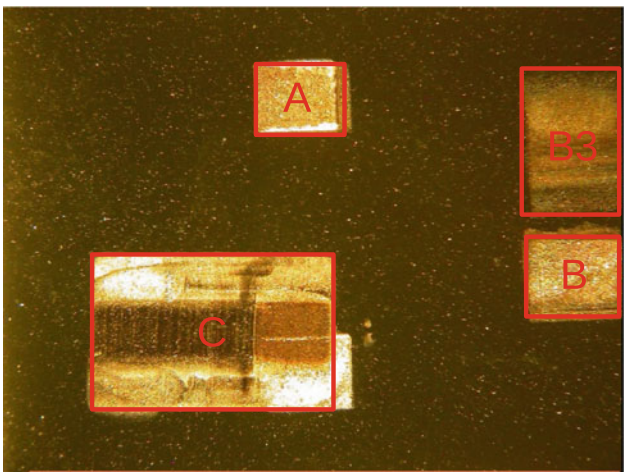

Fig. 2 Optical microscopy image of the polycrystalline CVD diamond thermal grade plate with dimensions that are (10 × 10 × 0.2) mm. The *black pads*, selected with *red rectangles*, are photogenerated layers with different laser parameters as explained in the text

3 Results and discussion

Recalling the main features of Raman spectra for CVD diamond and for any carbonaceous material, diamond shows a sharp peak centered at 1,332 cm^{-1}. The peak width is associated with the random stress, while the directional stress is associated with the peak shifting or splitting. In any carbonaceous material, the presence of trigonally coordinated carbon (graphite) with different degrees of structural disorder is associated with the G band about 1,580 cm^{-1}, the D (disorder) band about 1,350 cm^{-1} and the G' band about 2,720 cm^{-1}, with a shoulder at lower wavenumbers which is best defined in highly oriented pyrolytic graphite (HOPG), at about 2,680 cm^{-1}.

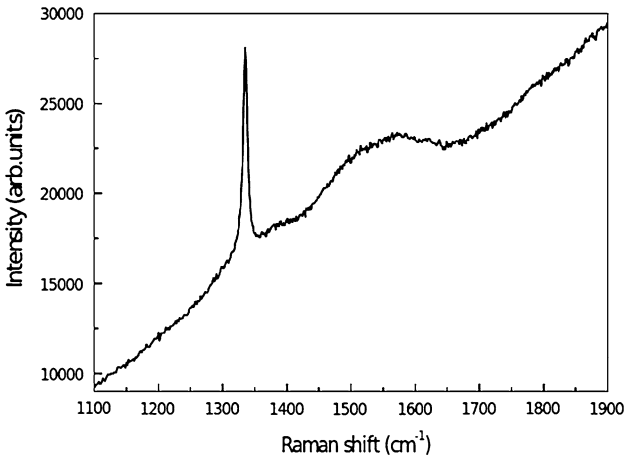

Fig. 3 Raman spectrum of unirradiated diamond

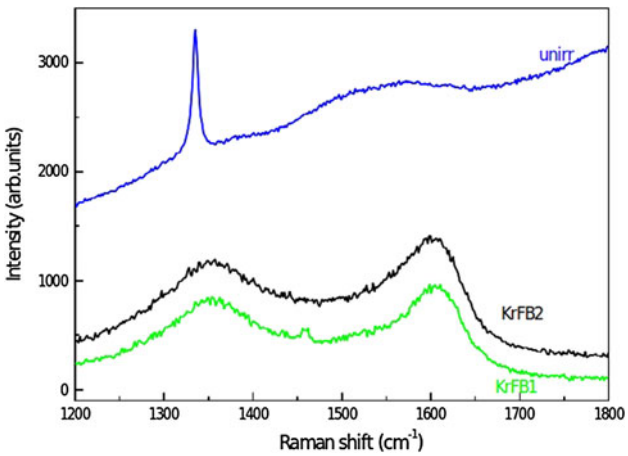

Fig. 6 Raman spectra taken at two different positions on B area (*KrFB1* and *KrFB2*), and on unirradiated diamond

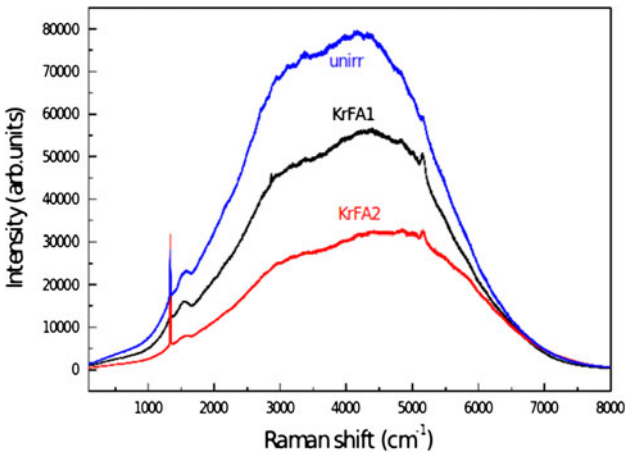

Fig. 4 PL spectra taken at two different positions on A area (*KrFA1* and *KrFA2*), and PL spectrum of unirradiated diamond

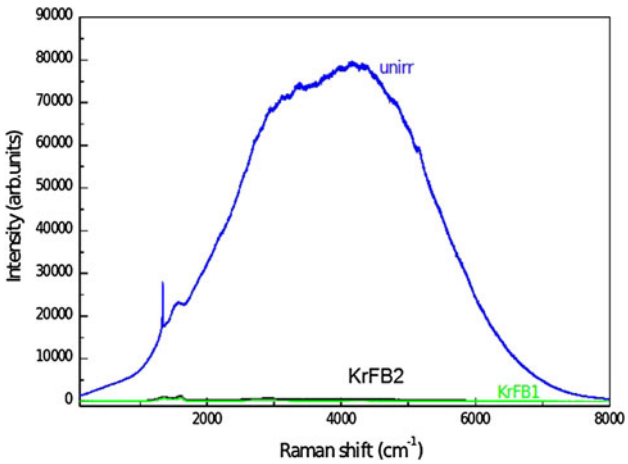

Fig. 7 PL spectra taken at two different positions on B area (*KrFB1* and *KrFB2*), and on unirradiated diamond

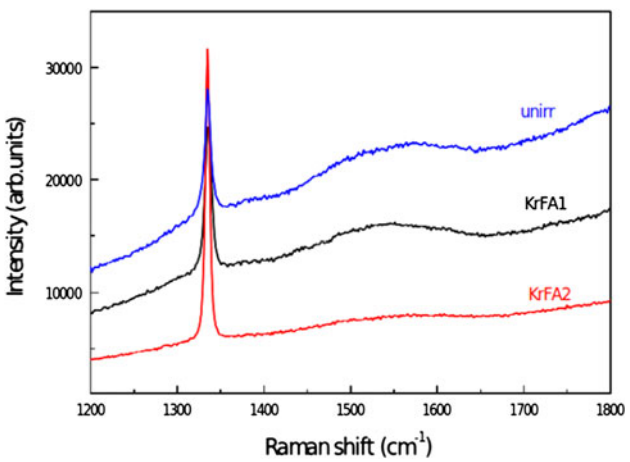

Fig. 5 Raman spectra taken at two different positions on A area (*KrFA1* and *KrFA2*) and on unirradiated diamond

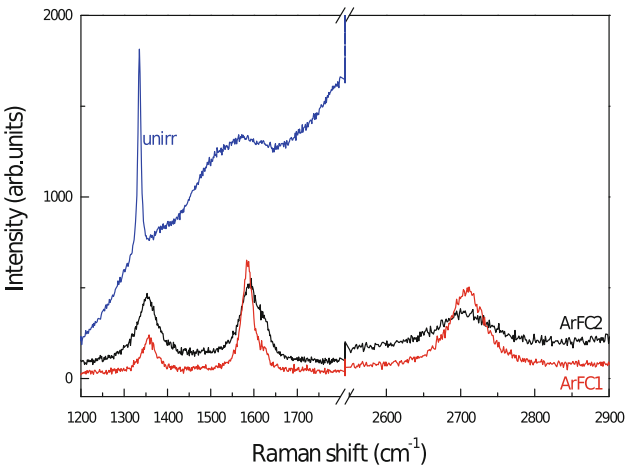

Fig. 8 Raman spectra taken at two different positions on the C area (*ArFC1* and *ArFC2*), and on unirradiated diamond

The last feature is nearly absent in turbostratic t-graphite, where the stacking of graphene layers is rotationally located with random angles along the c axis, and the G' band is a single Lorentian, like in a graphene monolayer (ML). Different materials present different FWHM values of G' bands with the same lineshape: 50–75 cm^{-1} is typical for t-graphite, while 25 cm^{-1} for graphene ML [2]. Another feature of CVD diamond is a high wavenumber contribution from vibronic centers which generates the PL intense band extending from about 3,000 to about 7,000 cm^{-1}, with a broad maximum around 5,000 cm^{-1} [3].

A typical Raman spectrum of the unirradiated diamond (Fig. 3) shows a narrow peak which is centered at 1,335 cm^{-1} (FWHM, 9 cm^{-1}) and a broad G band extending from about 1,450 to 1,650 cm^{-1}, with a maximum approximatively at 1,570 cm^{-1}; both these features grow up from a luminescence background. The G band is most likely due to the presence of graphitic carbon structures in CVD diamond [4]. At higher wavenumbers (Fig. 4), a complete spectrum of the unirradiated material is reported where the broad, intense PL band is the dominant feature. Here, we observe a very weak and characteristic feature at about 3,750 cm^{-1}, ascribed to the neutral (2.156 eV) charge state of a vacancy trapped at a single substitutional nitrogen which was accidentally incorporated in the material during the synthesis procedure [5]. Since the large wavenumber separation and intensity difference between Raman and PL features in all recorded spectra, we separately discuss both regions for our samples. From A area, we collected two Raman spectra at different positions, as shown in Fig. 5 (KrFA1 and KrFA2, respectively). These spectra show the same features of the unirradiated diamond ones. That can be explained because we irradiated the diamond plate with 200 consecutive laser pulses, and it is known that KrF laser starts graphitizing diamond surface but, continuing the irradiation, the laser can be absorbed by graphite, forcing it to evaporate [6]. Moreover, the G band maximum shifts weakly at about 1,545 cm^{-1} as evident in KrFA1, the band peak value lowers in KrFA2, and the diamond peak value (1,335 cm^{-1}) increases. It is well known that decreasing the graphite content (G band) in diamond film correspondingly diamond peak value will increase, [4]. In the same way, the PL bands (Fig. 4) keep the lineshape unaltered.

In the B area, we chose two points (KrFB1 and KrFB2) near the lower and upper borders of the irradiated area B. The Raman spectra from B area are exposed in Fig. 6. The bands at about 1,350 cm^{-1} (D) (very weak) and 1,590 cm^{-1}(G), emerging over a luminescence background, are most evident in the spectra of KrFB1 and KrFB2, exhibiting evident features of disordered graphite. In order to complete the observations, PL spectra were

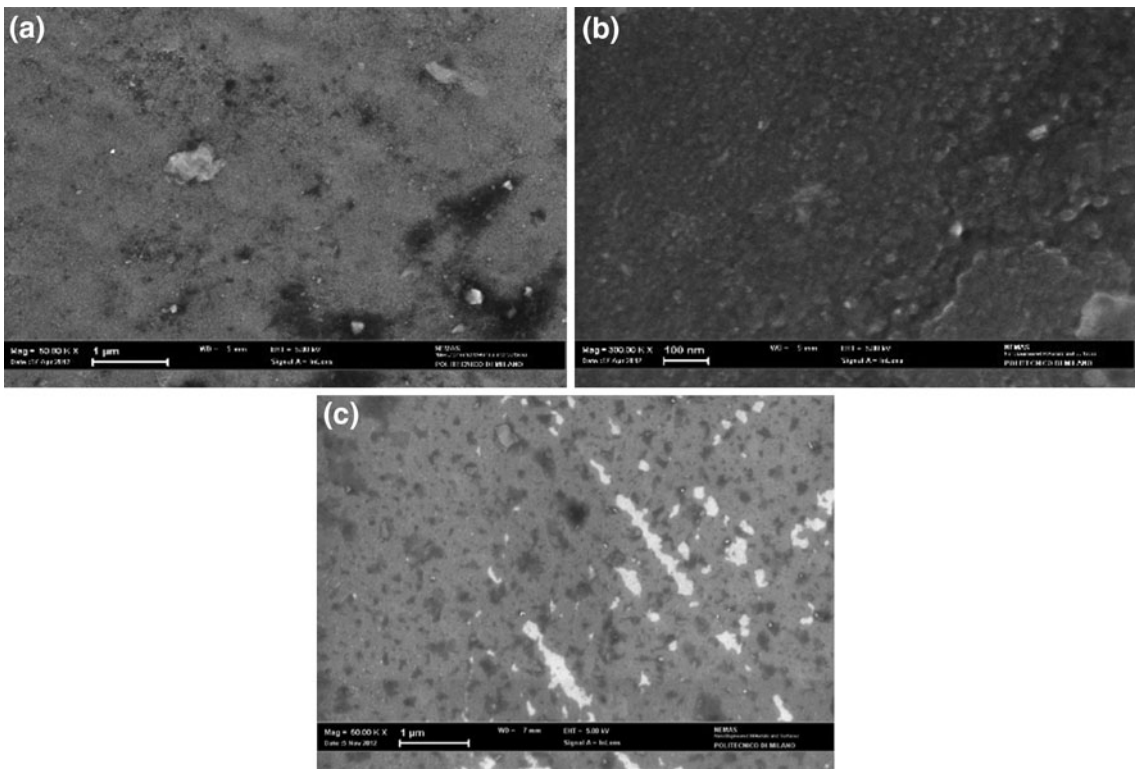

Fig. 9 SEM micrograph from B area at increasing magnification from **a** to **b**. In **c,** the unirradiated diamond surface is reported

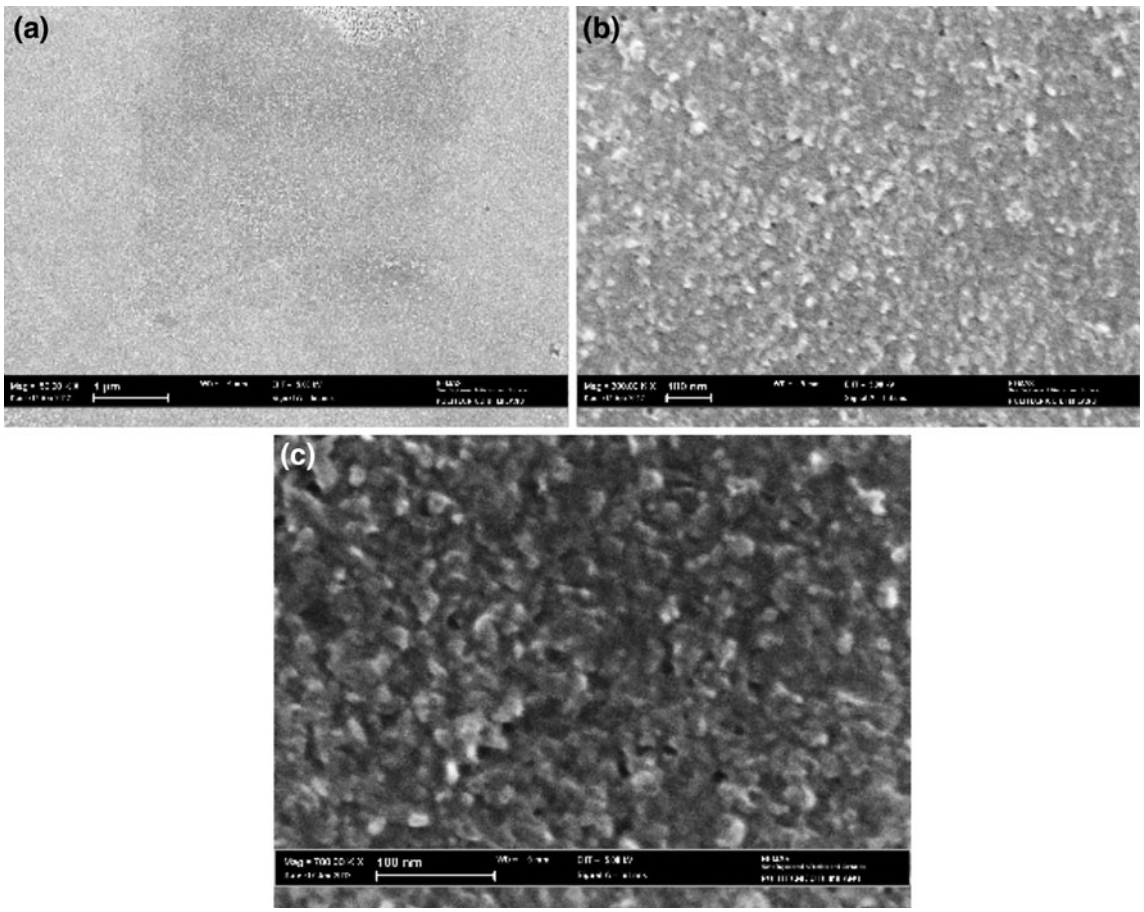

Fig. 10 SEM micrographs from C area at increasing magnifications from **a** to **c**

carried out on the same points (Fig. 7) and for curves labelled KrFB1 and KrFB2 tipical diamond band (blue curve in Fig. 7) disappear. This is another confirmation about the results obtained by Raman spectra in Fig. 6. The Raman spectra of C area are shown in Fig. 8. which reports deep changes on respect of unirradiated diamond and B area. The diamond features strongly decrease: the G band about 1,580 cm^{-1} is well defined, becoming sharper and sharper and more intense, while the D band at 1,360 cm^{-1} is less pronounced, see ArFC1 spectrum. Moreover, a second-order G' band appears centered at about 2,720 cm^{-1} with a single Lorentian lineshape and a FWHM of about 70 cm^{-1} for ArFC1 and about 110 cm^{-1} for ArFC2, while it is not possible to detect a PL band for C area. All the Raman measurements point out that ArF laser irradiation induces structural changes from diamond to disordered graphite (B areas) or to t-graphite (C area). To confirm the aforementioned results, we performed SEM observations. Fig. 9a, b are reported representative nanostructures of points B, while in Fig. 9c, the unirradiated diamond surface is reported as comparison. At low magnification (Fig. 9a), the laser-irradiated surface looks quite homogeneous, with some scattered debris, sized 0.2–0.5 μm; at higher magnification (Fig. 9b), the surface appears to consist of a homogeneous distribution of irregularly shaped particles, with average size around 20–30 nm. Pictures taken from C area are showed in Fig. 10. At higher magnification, we can observe at first a surface homogeneously modified by the laser radiation (Fig. 10a). The details of a randomly oriented distribution with irregularly shaped flakes, partly protruding outwards from the surface become evident and constitute a signature of t-graphite (Fig. 10b); increasing the magnification (Fig. 10c), the flakes are even more clearly visible and their average size can be estimated around 20–30 nm. Such morphology was observed only in C area. CVD diamond has an energy gap of 5.5 eV (225 nm), so ArF laser ($\lambda = 193$ nm, $E = 6.45$ eV) is better absorbed than radiation from KrF laser ($\lambda = 248$ nm, $E = 5.0$ eV), and it could explain the different behaviors of diamond at the two wavelengths [6].

4 Conclusions

In this paper, we irradiated a CVD diamond plate by using an excimer laser working at two different wavelengths: 248

and 193 nm. The irradiated areas were characterized by micro-Raman and PL measurements, then the results were compared with images obtained by SEM. Using KrF laser, at best, we obtained only disordered graphite; indeed from the micro-Raman D band and G band spectra, it is possible to observe a graphite layer when the surface is irradiated with only 10 laser pulses, while the graphite layer seems to disappear with 200 consecutive laser pulses because of the ablation process, which is a competitor of the graphitization process, starts to become predominant. Using ArF laser, the micro-Raman measurements point out a spectrum having single Lorentzian peak at 2,720 cm^{-1} with an associated FWHM of about 90 cm^{-1} which is an intermediate value from two measurements collected from two different points of the same layer. The FWHM value means that the surface modified layer is formed by a turbostratic graphite layer. SEM observations confirm our results. Increasing the magnification, we observe the distribution of randomly oriented, clearly visible and irregularly shaped flakes, partly protruding outwards from the surface, being a signature of a t-graphite layer, and their average size can be estimated about 20–30 nm.

Acknowledgments The support of INFN Technology and Interdisciplinary National Scientific Committee (CSN5) through the experiment DIAPIX (DIAmondPIXel) is acknowledged.

References

1. C. Canali, E. Gatti, S.F. Kozlov, P.F. Manfredi, C. Manfredotti, F. Nava, A. Quirini, Electrical properties and performances of natural diamond nuclear radiation detectors. Nucl. Instrum. Methods **160**, 73 (1979)
2. L.M. Malard, M.A. Pimenta, G. Dresselhaus, M.S. Dresselhaus, Raman spectroscopy in graphene. Phys. Rep. **473**, 51–87 (2009)
3. A.T. Collins, in *The Physics of Diamond*, ed. by A. Paoletti, A. Tucciarone (IOS Press, Oxford, 1997), p. 273
4. L. Nistor, V. Ralchenko, I. Vlasov, A. Khomich, R. Khmelnitskii, P. Potapov, J. Van Landauyt, Formation of amorphous carbon and graphite in CVD diamond upon annealing: a HREM, EELS, Raman and optical study. Physica Status Solidi A **186**(2), 207–214 (2001)
5. K. Iakoubovskii, G.J. Adriaenssens, Photoluminescence in CVD diamond films. Physica Status Solidi A **172**(1), 123–129 (1999)
6. V.N. Strekalov, V.I. Konov, V.V. Kononenko, S.M. Pimenov, Early stages of laser graphitization of diamond. Appl. Phys. A **76**, 603–607 (2003)